UCRL 3571
c.8

UNIVERSITY OF CALIFORNIA

Radiation Laboratory

TWO-WEEK LOAN COPY

This is a Library Circulating Copy which may be borrowed for two weeks. For a personal retention copy, call Tech. Info. Division, Ext. 5545

BERKELEY, CALIFORNIA

DISCLAIMER

This document was prepared as an account of work sponsored by the United States Government. While this document is believed to contain correct information, neither the United States Government nor any agency thereof, nor the Regents of the University of California, nor any of their employees, makes any warranty, express or implied, or assumes any legal responsibility for the accuracy, completeness, or usefulness of any information, apparatus, product, or process disclosed, or represents that its use would not infringe privately owned rights. Reference herein to any specific commercial product, process, or service by its trade name, trademark, manufacturer, or otherwise, does not necessarily constitute or imply its endorsement, recommendation, or favoring by the United States Government or any agency thereof, or the Regents of the University of California. The views and opinions of authors expressed herein do not necessarily state or reflect those of the United States Government or any agency thereof or the Regents of the University of California.

UCRL-3571

UNIVERSITY OF CALIFORNIA

Radiation Laboratory
Berkeley, California

Contract No. W-7405-eng-48

COMPARISON OF THE REACTIONS

$$p + d \longrightarrow H^3 + \pi^+,$$

$$p + d \longrightarrow He^3 + \pi^0$$

AS A TEST OF CHARGE INDEPENDENCE

Kenneth C. Bandtel, Wilson J. Frank,
and Burton J. Moyer

Printed for the U. S. Atomic Energy Commission

COMPARISON OF THE REACTIONS $p + d \longrightarrow H^3 + \pi^+$, $p + d \longrightarrow He^3 + \pi^0$ AS A TEST OF CHARGE INDEPENDENCE

Kenneth C. Bandtel, Wilson J. Frank, and Burton J. Moyer

Radiation Laboratory
University of California
Berkeley, California

October 26, 1956

ABSTRACT

The pair of reactions indicated above have been investigated experimentally to see if the predictions of the theory of charge independence are fulfilled. Because of the low cross section (a few microbarns) and large background (heavy particles emitted at $\sim 10^\circ$ lab) the results do not provide as critical a test as might be hoped. We find that there is a 50% chance that the ratio of the reaction cross sections $(p + d \longrightarrow \pi^+ + H^3) / (p + d \longrightarrow \pi^0 + He^3)$ is between 2.01 and 2.63. Charge independence predicts that the ratio should be exactly two. The experimental difficulties would be less at higher proton energies; this method would seem to provide a very stringent test of charge independence if the comparison could be made with sufficient accuracy.

COMPARISON OF THE REACTIONS $p + d \longrightarrow H^3 + \pi^+$, $p + d \longrightarrow He^3 + \pi^0$ AS A TEST OF CHARGE INDEPENDENCE *

Kenneth C. Bantel,+ Wilson J. Frank,+
and Burton J. Moyer

Radiation Laboratory
University of California
Berkeley, California

October 26, 1956

INTRODUCTION

A study comparing the reactions

$$p + d \longrightarrow t + \pi^+ \quad \text{and}$$

$$p + d \longrightarrow He^3 + \pi^0$$

would provide information for a stringent test of the hypothesis of charge independence of nuclear forces.[1,2]

Other experimental investigations of this hypothesis have been concerned with the reaction pair, $p + p \longrightarrow \pi^+ + d$ and $n + p \longrightarrow \pi^0 + d$. Hildebrand measured the angular distribution of the $n + p \longrightarrow \pi^0 + d$ reaction;[3] Durbin, Loar and Steinberger measured $d + \pi^+ \longrightarrow p + p$ for the same center of mass (c.m.) energy.[4] Both results closely fit the same angular distribution (i.e.

---

* This work was done under the auspices of the U. S. Atomic Energy Commission.

+ Now at Radiation Laboratory, University of California, Livermore, California.

1 A. M. L. Messiah, Phys. Rev. 86, 430 (1952).

2 M. Ruderman, Phys. Rev. 87, 383 (1952).

3 R. H. Hildebrand, Phys. Rev. 98, 1090 (1953).

4 Durbin, Loar, and Steinberger, Phys. Rev. 84, 581 (1951).

$0.2 + \cos^2 \theta$), in agreement with the predictions of charge independence. R. A. Schluter measured the $n + p \rightarrow \pi^0 + d$ reaction for incident neutron energies near 400 Mev.[5] He found the total cross section by integration (at a given c.m. energy) and compared twice the value with various total cross-section measurements of the $p + p \rightarrow \pi^+ + d$ reaction that have been made in this energy range. Schluter's data are based on 102 deuterons; total cross section and energy dependence are in agreement with the π^+ experiment within the accuracy of the data.

The experimental results in this paper were obtained during the spring and summer of 1954. In mid 1955, the experiment was intensively pursued again with various improvements and changes in instrumentation. Unfortunately the early results were not improved upon, because of the inherent experimental difficulties stemming from measuring a very low cross section (about a microbarn), with reaction products coming out at less than 10° from the beam direction.

5. R. A. Schluter, Phys. Rev. 96, 734 (1954).

II. EXPERIMENTAL DETAILS

A. Method

A liquid deuterium target was bombarded by 340-Mev protons from the Berkeley 184 inch synchrocyclotron. The heavy particles, H^3 and He^3, are identified by measuring $\frac{dE}{dx}$ and E at the expected angle. The π^+ is detected at its expected angle; the difference in time of flight[6] between it and the H^3 helps to identify the $p + d \longrightarrow H^3 + \pi^+$ process. The π^0 is not detected because of uncertainties in the efficiency of a gamma-ray counter, and because of the spreading of photons in the π^0 decay. The $p + d \longrightarrow He^3 + \pi^0$ process is identified only by the He^3 energy and ionization rate.

The two heavy particles are detected concurrently in a "heavy-particle telescope" consisting of three plastic scintillators (Fig. 1). The first scintillator is the $\frac{dE}{dx}$ counter for He^3; the second serves as both the He^3 E and the H^3 $\frac{dE}{dx}$ counter; the third scintillator is the H^3 E counter. For He^3 particles, a double coincidence is required between the first two scintillators. For H^3 particles a triple coincidence is required between the π^+ meson counter, delayed (owing to the H^3 time of flight), and the second and third scintillators of the telescope. The two types of events are measured concurrently, so that alternate runs to measure each process are not needed.

Each of the scintillators is viewed separately by 1P21 and 5819 photomultiplier tubes. The second scintillator is viewed by a double set of tubes for independent control of the H^3 and He^3 detection networks. The 5819 tubes provide pulse-height signals, and the 1P21 tubes provid signals for the

---

6. Frank, Bandtel, Madey, and Moyer, Phys. Rev. 94, 1716 (1954).

The vacuum jacket around the deuterium container (in which the deuterium is condensed by liquid hydrogen) is essential for providing heat insulation. The vacuum pipe for the scattered particles is necessary to prevent bad multiple scattering of the 85-Mev He^3 particles in air. Furthermore, it was found from a preliminary run that a 20-mil dural window in the beam exit tube, the intervening air, and an entrance foil in the target enclosure all contributed appreciably to the background; therefore it was clearly desirable to provide the essentially complete vacuum path as shown. Since the thickness of the liquid deuterium plus the foils that contain the liquid deuterium is limited to about 0.09 g/cm^2 by multiple-scattering requirements for the He^3 particle, it can be seen that even the two 1-mil foils that contain the liquid deuterium (0.04 g/cm^2) contribute appreciably to the background. The low differential cross section (only a few microbarns) intensifies this problem.

C. Geometry and Kinematics

As shown on the experimental arrangement in Fig. 3, the heavy-particle telescope angle was 10.5°, and the correlated angle for the π^+ particle was 37°. Because of the $\pi^+ - \pi^0$ mass difference, the kinematics for the two reactions transform differently from the laboratory to the center-of-mass system. For the triton, 10.5° in the laboratory system corresponds to 129.03° in the center-of-mass system; for the He^3, 10.5° lab corresponds to 134.35° c.m. Because of this effect, the experimentally measured ratio has to be corrected in accordance with the previously measured[6] angular distribution for the $p + d \rightarrow \pi^+ + H^3$ reaction so that the same c.m. angle is compared for both reactions.

III. RESULTS OF THE EXPERIMENT

A. Reduction of Data

1. He^3 Particles

Figure 4 shows the results of plotting the pulse height in the first scintillator vs the pulse height in the second scintillator, considering only those particular cases in which the particle stopped in the second scintillator. The scintillator thicknesses have been arranged so that He^3 particles of the expected energy (85 Mev) should stop in the second scintillator. Many more pulses passed through into the third scintillator than stopped in the second. Many slow protons and other singly charged particles would appear in the lower left corner of the plot, but they all enter the third scintillator and so have not been plotted. The gains and voltages were set so that 85-Mev He^3 particles would appear at approximately (10,10). This was accomplished by a preliminary calibration on the He^3 beam of the 184-in. cyclotron, which was degraded in energy. The degrading absorber was placed in the emergent beam of He^3 particles just after they were deflected from their cyclotron orbit, and the steering-magnet current was lowered to direct the 85-Mev He^3 particles into the experimental area. Calibration data showed that most of the He^3 particles should fall within ± 25% of the centroid of the distribution. This is approximately true for the pulse height in the first scintillator. The pulse height in the second scintillator spreads more than this, owing to the spread in energy in escaping from different parts of the target.

It seems extremely probable that the events in the center of the plot represent He^3 or He^4 particles. However, He^4 particles could not be

produced by bombarding deuterium by protons, and any He^4 particles produced from the foils are subtracted out in getting the difference counting rate. The final results are:

	Counts	Units of integrated beam	Counts per unit of integrated beam
Full target	178	10.56	-------
Empty target	36	6.29	-------
Difference (liquid deuterium target)	---	----	11.2 ± 1.6

Blank runs were accomplished by closing the exhaust valve above the target vessel, and slightly warming the latter electrically, so that the liquid phase was forced back out of the target into a reservoir by the pressure of deuterium vapor. It is estimated that the blank represents ~2% of the amount of deuterium contained when liquid deuterium filled the target (the presence of the foils contributes a background of about 30%).

2. H^3 Particles

Figures 5 and 6 show the results of plotting pulse heights No. 3 ($H^3 \frac{dE}{dx}$, Scintillator 2) and No. 4 (H^3 E, Scintillator 3) for the full- and empty-target runs. (Although Pulses 2 and 3 are both proportional to the light in the second scintillator, the He^3 E pulse is almost an order of magnitude larger than the $H^3 \frac{dE}{dx}$ pulse. Since the dynamic range of the 517 scope vertical amplifier is just about an order of magnitude, two separate gain controls are necessary.) At first glance it is clear that a certain region of the full-target plot is more densely populated than in the empty-target plot; placing a line of demarcation, however, requires much consideration.

Figure 7 shows a plot of relative energy loss for protons, deuterons, and tritons in the second and third scintillators. Because of saturation

effects when specific ionization is high (particle energy is low), an expected pulse-height plot would be considerably modified. The light produced per Mev of energy loss as a function of specific ionization is given in Fig. 8; this curve is derived from experimental data for a number of phosphors, but does not include our scintillator material —$(C_2H_2)_n$ plus a trace of terphenyl. It is assumed that saturation effects do not differ greatly from one organic scintillator to another.

Figure 8 may be transformed into the curves of Figure 9 by use of the relation for dT/dx vs T for $(C_2H_2)_n$. From integration over appropriate intervals of T under the curves of Fig. 9 we obtain the plots of relative light output in Fig. 10 corresponding to the relative energy losses shown in Fig. 7 for the phosphors employed. The curves of Fig. 10 would describe the distributions in Figs. 5 and 6 if resolution were perfect and light outputs were unique for similar events.

The H^3 pulse height counters were calibrated by using deuterons of such an energy as to give the same $\frac{dE}{dx}$ pulse as the expected tritons. The tritons were expected to fall around (10,10), but instead they appear centered about (8,9). By a cut-and-try process, the information from Fig. 10 has been fitted to the data in Figs. 5 and 6. The lines on Figs. 5 and 6 are isomass lines, representing the probable particle mass in multiples of the proton mass.

In Fig. 11, the number of particles per mass interval has been plotted against the mass; the cut-and-try procedure of calibrating the data involved centering the scattered proton peak around the proton mass location. Clearly, there are a number of mass-3 particles.

The triton peak can be seen more clearly by plotting the difference-counting ratio per isomass interval (Fig. 12). The whole length of the isomass

interval has been included. Since the tritons have an expected energy of 37 ± 10 Mev, the two dotted lines in Figs 5 and 6 represent the expected limits. Figure 13 is a replot of Fig. 12 with the restricted triton data. Summed over these counts, the triton counting rate is 32.0 ± 2.7.

As another attempt to separate the tritons from the background particles, two ovals have been drawn, centered on (8,9). The inner oval represents the 100% resolution width determined by the calibration run, while the outer oval is 50% larger, allowing for a margin of error. The resulting counting rates are 28.7 ± 2.1 for the inner oval, and 31.5 ± 2.9 for the outer one.

The counting rate seems relatively insensitive to the separation criteria; the first one (32.0 ± 2.7 counts per unit of integrated beam) is used in subsequent calculations.

B. Results

The He^3 and H^3 particles were measured at 10.5°. This means the π^0 is at 45.65° c.m., and the π^+ is at 50.97° c.m. The measured angular distribution[6] of $p + d \longrightarrow t + \pi^+$ was used to correct the π^+ to the same c.m. angle as the π^0, since we must compare the same angles in the center-of-mass system in order to test charge independence:

$$\frac{\frac{d\sigma}{d\Omega_{cm}}(\pi^+, 45.7^\circ)}{\frac{d\sigma}{d\Omega_{cm}}(\pi^0, 45.7^\circ)} = \frac{\frac{d\sigma}{d\Omega_{cm}}(\pi^+, 51.0^\circ)}{\frac{d\sigma}{d\Omega_{cm}}(\pi^0, 45.7^\circ)} \times \frac{\frac{d\sigma}{d\Omega_{cm}}(\pi^+, 45.7^\circ)}{\frac{d\sigma}{d\Omega_{cm}}(\pi^+, 51.0^\circ)}$$

and

$$\text{Counting Rate} \sim \frac{d\sigma}{d\Omega_{cm}} \frac{d\Omega_{cm}}{d\Omega_{LAB}} \Delta\Omega_{LAB}$$

$$\frac{d\sigma}{d\Omega_{cm}} \sim \frac{CR}{\Delta\Omega_{LAB}} \left(\frac{d\Omega_{LAB}}{d\Omega_{cm}}\right).$$

Therefore we have

$$\frac{\frac{d\sigma}{d\Omega}(\pi^+, 45.7^\circ)}{\frac{d\sigma}{d\Omega}(\pi^\circ, 45.7^\circ)} = \underbrace{\frac{\left(\begin{matrix}\text{counting rate}\\ \text{per unit beam}\end{matrix}\right)_{\pi^+}}{\left(\begin{matrix}\text{counting rate}\\ \text{per unit beam}\end{matrix}\right)_{\pi^\circ}}}_{R_1} \times \underbrace{\frac{\frac{d\sigma}{d\Omega_{cm}}(\pi^+, 45.7^\circ)}{\frac{d\sigma}{d\Omega_{cm}}(\pi^+, 51.0^\circ)}}_{R_2} \times \underbrace{\frac{\left(\frac{d\Omega_{LAB}}{d\Omega_{cm}}\right)_{\pi^+, 51.0^\circ}}{\left(\frac{d\Omega_{LAB}}{d\Omega_{cm}}\right)_{\pi^\circ, 45.7^\circ}}}_{R_3}$$

R_1 is the raw data we get from the experiment. The error in this factor reflects the counting statistics of the experiment presented here.

R_2 is information we obtain from the previous experiment[6]. Unfortunately, we do not know this with much better accuracy than R_1. In order to get an estimate of R_2, we plotted the angular distribution data[6] and drew lines through the extremities of the probable errors. Then we read off values and probable errors at 45.7° and 51.0°, took the ratio, and compounded the error in the ratio, thus obtaining the value of R_2.

R_3 is just a matter of kinematical calculation. The following results were obtained:

$$R_1 = \frac{32.0\ (\pm\ 5.7\%)}{11.2\ (\pm\ 9.6\%)} = 2.86\ (\pm\ 11.2\%);$$

$$R_2 = \frac{2.90\ (\pm\ 6.2\%)}{2.47\ (\pm\ 4.1\%)} = 1.175\ (\pm\ 7.4\%);$$

$$R_3 = 1/38.6 \Big/ \frac{1}{26.7} = 0.692;$$

$$(R_1)(R_2)(R_3) = 2.32\ (\pm\ 13.4\%) \left\{\begin{matrix}2.63\\ 2.01\end{matrix}\right.$$

(Probable errors are quoted here).

C. Accuracy

A comparison experiment was done to minimize errors in beam monitoring, solid angle, etc. Nuclear interactions that result in the loss of the particle being detected are estimated to be negligible. In the thickest phosphor about 7% of the tritons suffer an inelastic nuclear interaction, and less than 7% are removed from the triton island, since an inelastic event does not always carry off energy in a way that does not produce light.

Consequently, it is believed that the biggest single contribution to the error is the counting statistics of this and the previous experiment.

D. Interpretation

The results of this experiment indicate there is a 50% chance that the ratio of the reaction cross sections $(p + d \rightarrow n^+ + H^3) / (p + d \rightarrow n^0 + He^3)$ is between 2.01 and 2.63.

The statistical accuracy of the experiment is regrettably poor, but this is for the most part due to the low cross section of the reaction, which intensifies the detection and background difficulties.

One would have to say that the results of this experiment are in accord with the predictions of the hypothesis of conservation of isotopic spin, but in view of its poor statistical accuracy, this experiment does not provide a critical test of the conservation of isotopic spin.

Fig. 10. Calculated light output from second phosphor vs that from third phosphor.

Fig. 11. Differential mass spectrum for second and third scintillators.

Fig. 12. Differential mass spectrum for second and third scintillators (full target) - (empty target) per unit of integrated beam.

Fig. 13. Differential mass spectrum $\frac{\text{(full target) - (empty target)}}{\text{unit integrated beam}}$ vs ISO mass interval.

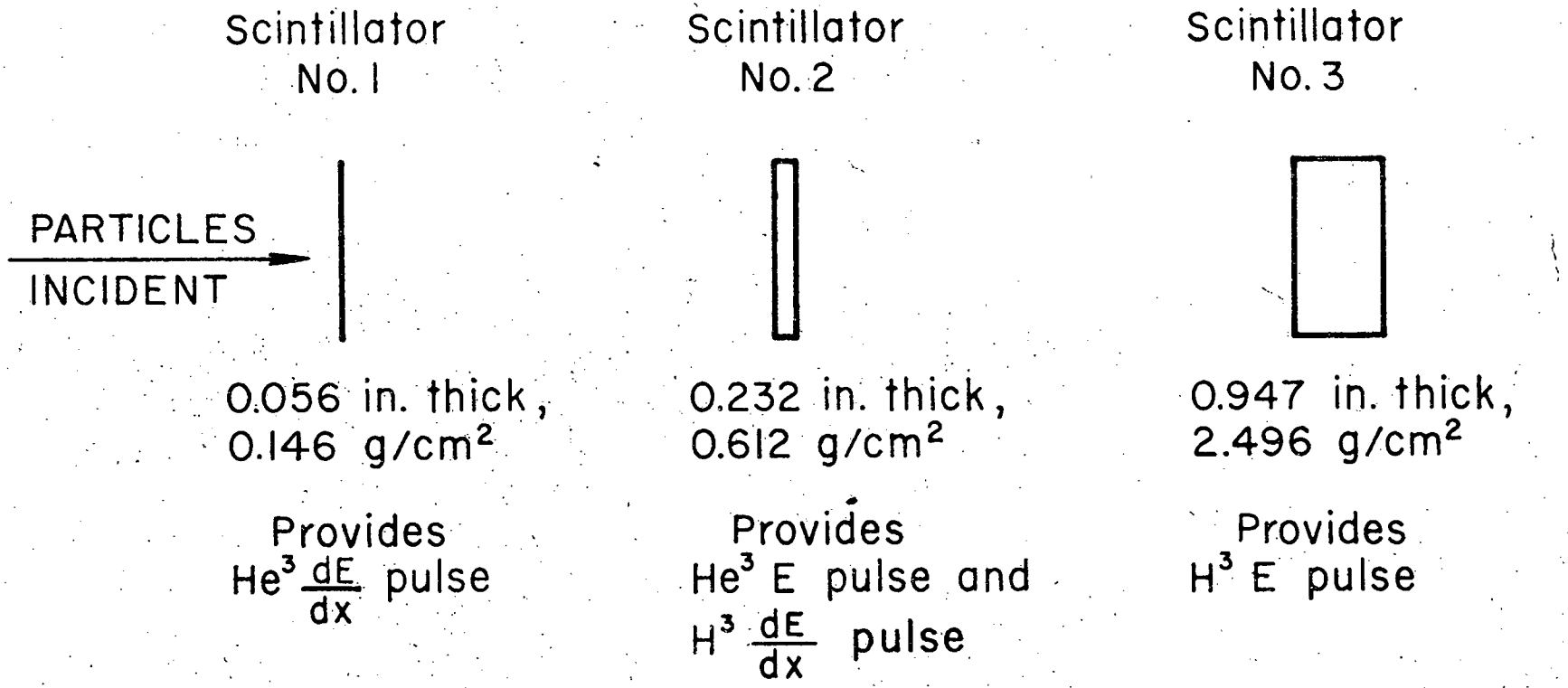
Scintillator No. 1
Scintillator No. 2
Scintillator No. 3
PARTICLES INCIDENT
0.056 in. thick, 0.146 g/cm²
0.232 in. thick, 0.612 g/cm²
0.947 in. thick, 2.496 g/cm²
Provides He³ dE/dx pulse
Provides He³ E pulse and H³ dE/dx pulse
Provides H³ E pulse

Fig 1

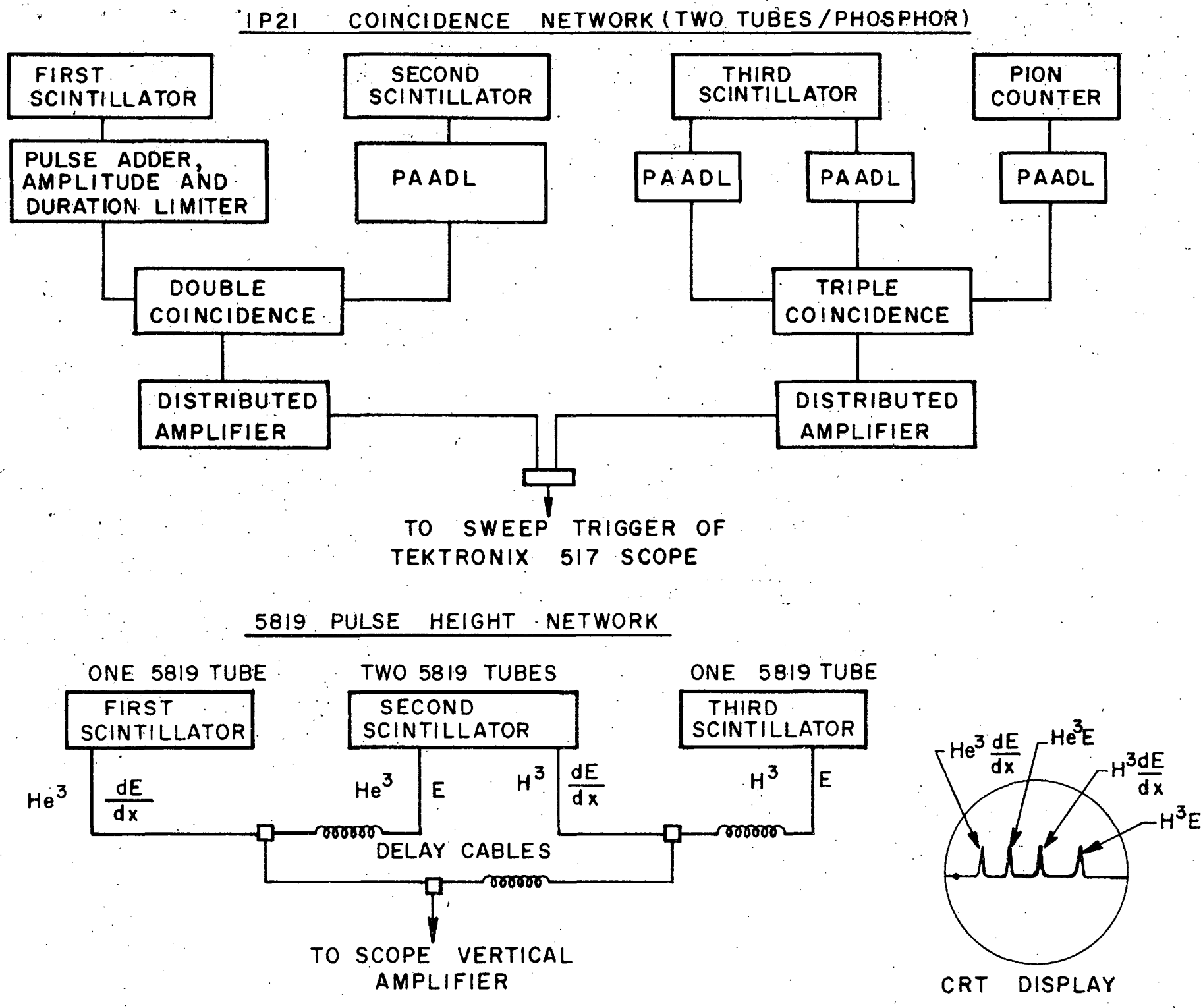

Block Diagram of Electronics

Fig 2

22463-1

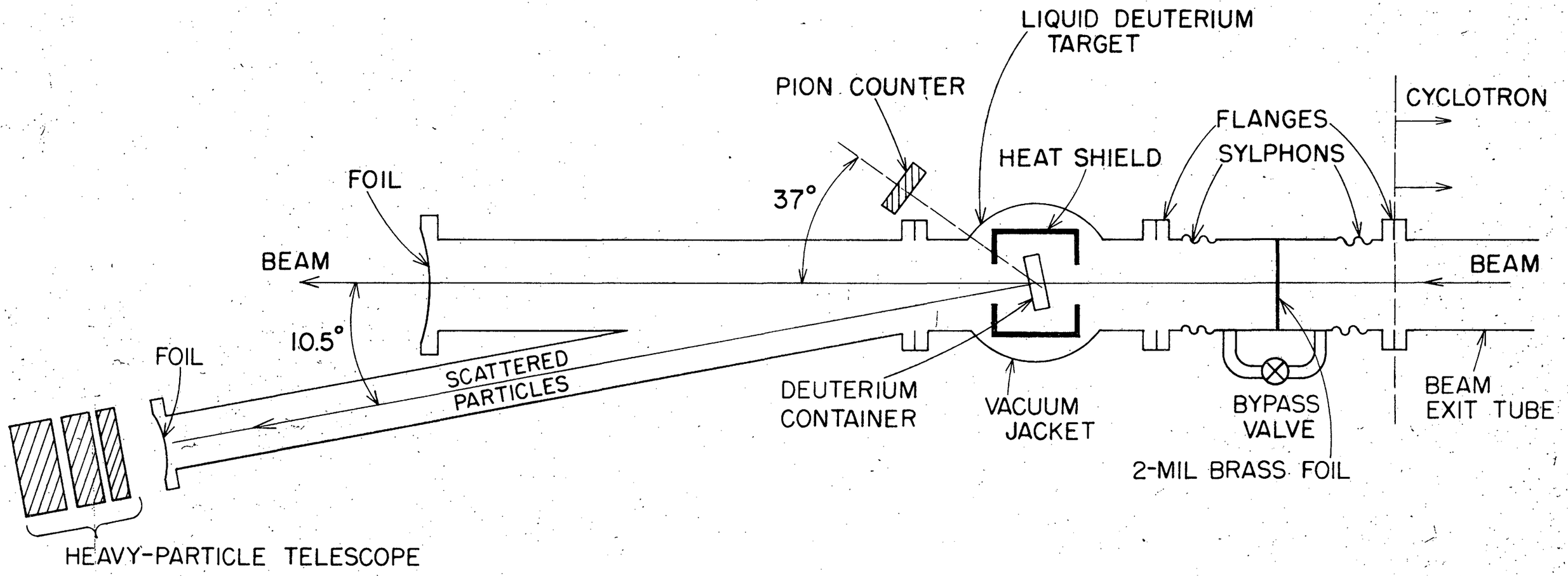
LIQUID DEUTERIUM TARGET
PION COUNTER
CYCLOTRON
FLANGES
SYLPHONS
HEAT SHIELD
FOIL
37°
BEAM
BEAM
10.5°
FOIL
SCATTERED PARTICLES
DEUTERIUM CONTAINER
VACUUM JACKET
BYPASS VALVE
BEAM EXIT TUBE
2-MIL BRASS FOIL
HEAVY-PARTICLE TELESCOPE

Fig 3

226322

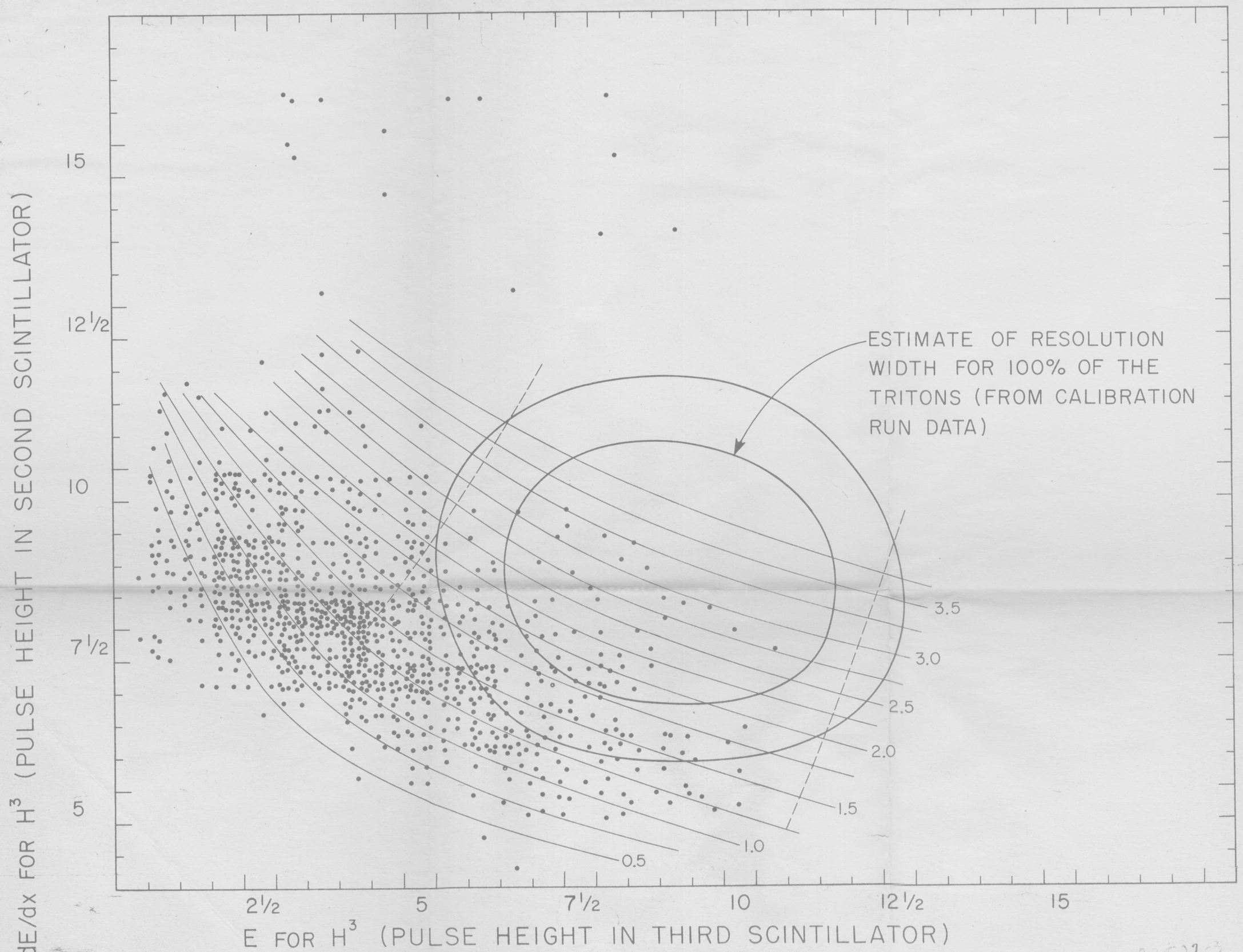
ESTIMATE OF RESOLUTION WIDTH FOR 100% OF THE TRITONS (FROM CALIBRATION RUN DATA)
3.5
3.0
2.5
2.0
1.5
1.0
0.5
15
12 1/2
10
7 1/2
5
2 1/2
5
7 1/2
10
12 1/2
15
dE/dx FOR H3 (PULSE HEIGHT IN SECOND SCINTILLATOR)
E FOR H3 (PULSE HEIGHT IN THIRD SCINTILLATOR)

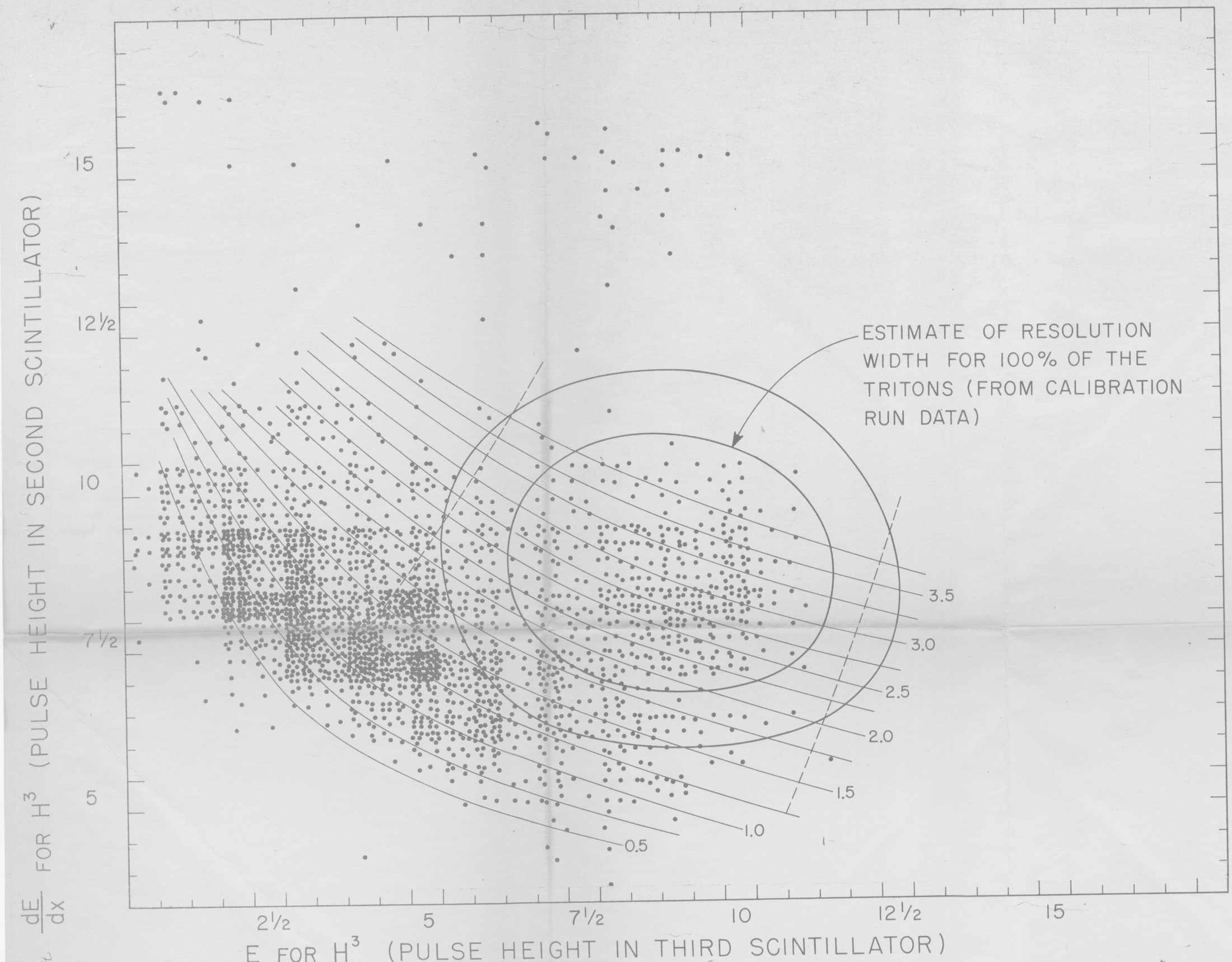
ESTIMATE OF RESOLUTION WIDTH FOR 100% OF THE TRITONS (FROM CALIBRATION RUN DATA)
3.5
3.0
2.5
2.0
1.5
1.0
0.5
15
12½
10
7½
5
2½
5
7½
10
12½
15
dE/dx FOR H³ (PULSE HEIGHT IN SECOND SCINTILLATOR)
E FOR H³ (PULSE HEIGHT IN THIRD SCINTILLATOR)

22526-3

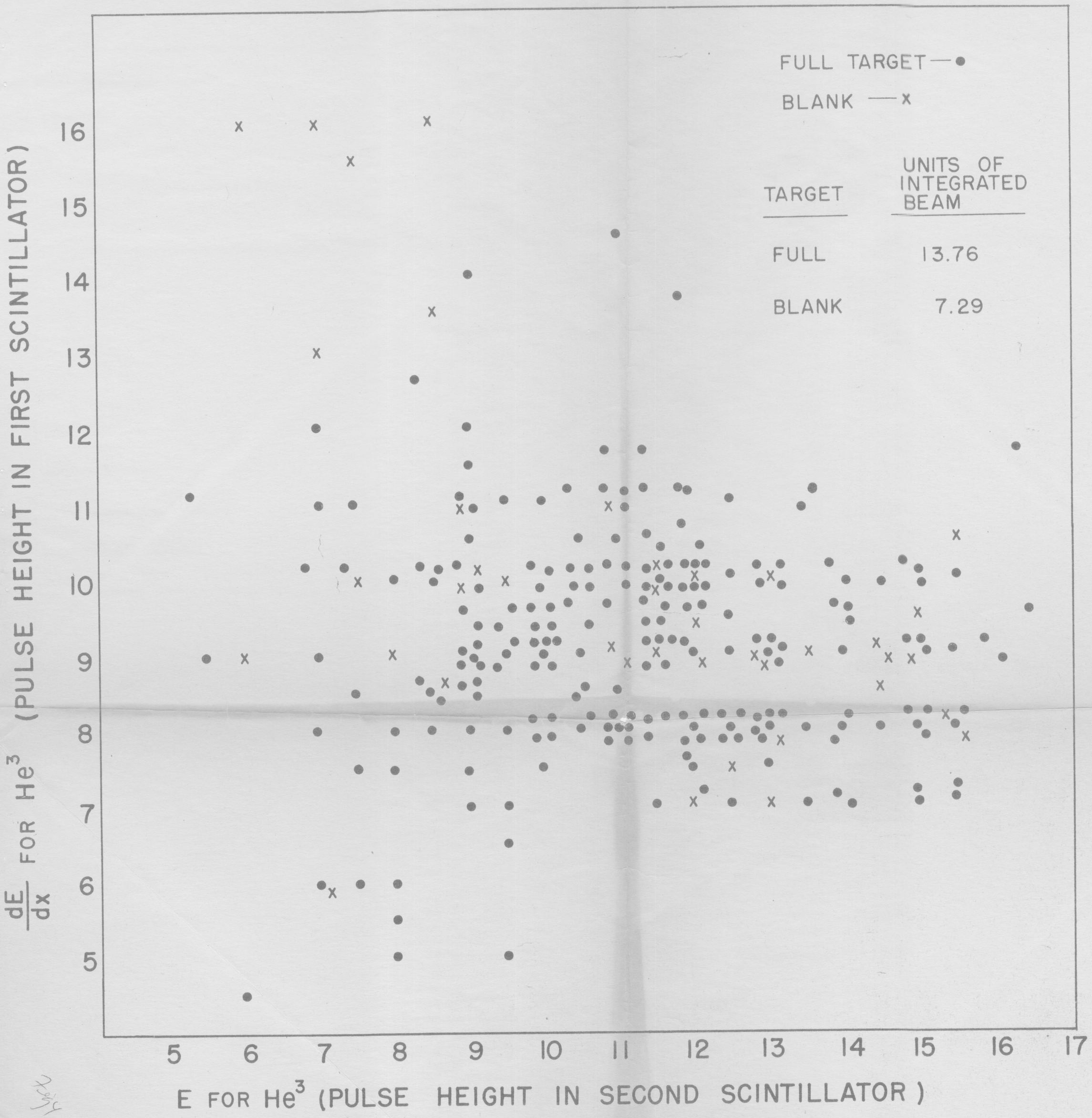
FULL TARGET — ●
BLANK — x
TARGET
UNITS OF INTEGRATED BEAM
FULL 13.76
BLANK 7.29
dE/dx FOR He3 (PULSE HEIGHT IN FIRST SCINTILLATOR)
E FOR He3 (PULSE HEIGHT IN SECOND SCINTILLATOR)
5 6 7 8 9 10 11 12 13 14 15 16 17
5 6 7 8 9 10 11 12 13 14 15 16

22462-3

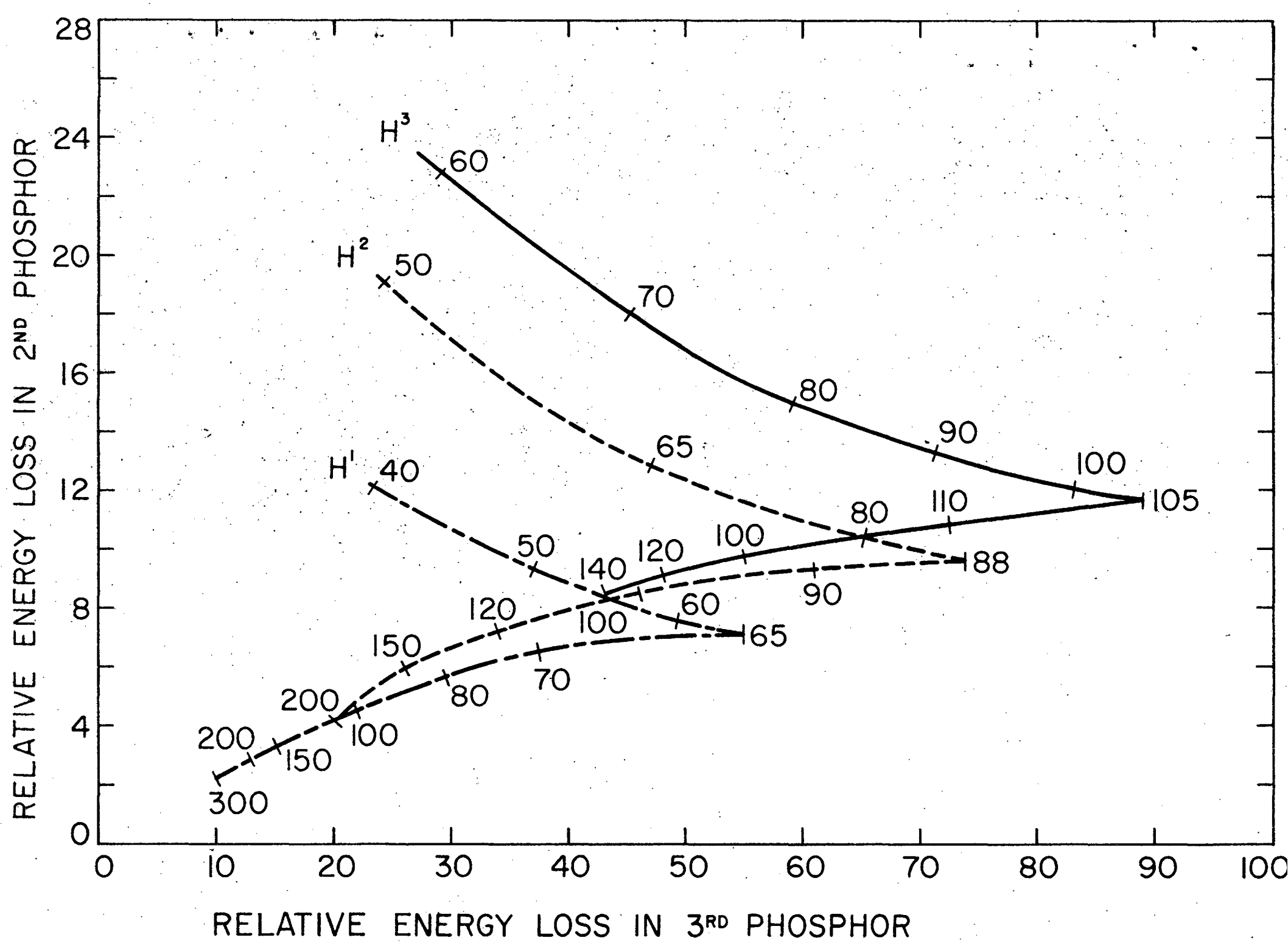

RELATIVE ENERGY LOSS IN 2ND PHOSPHOR
RELATIVE ENERGY LOSS IN 3RD PHOSPHOR
H3
H2
H1
60
70
80
90
100
105
50
65
88
40
50
140
120
100
80
110
90
60
65
120
100
150
70
80
200
100
200
150
300
0
4
8
12
16
20
24
28
0
10
20
30
40
50
60
70
80
90
100

Fig 7

23801-1

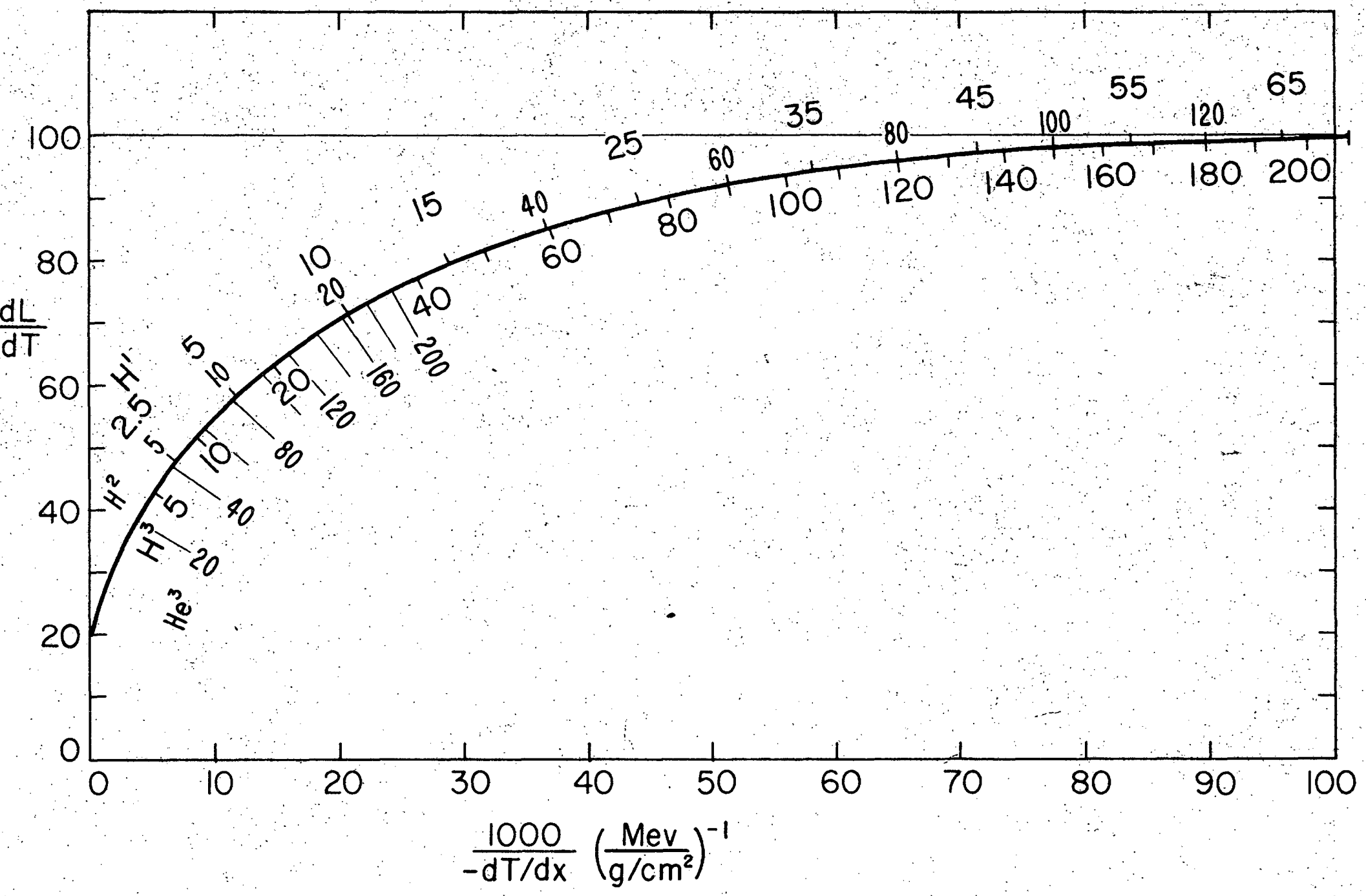
dL/dT
100
80
60
40
20
0
0
10
20
30
40
50
60
70
80
90
100
1000/(-dT/dx) (Mev/g/cm²)^-1
H'
H²
H³
He³
2.5
5
10
20
40
80
120
160
200
15
25
35
45
55
65

Fig 8

23803-1

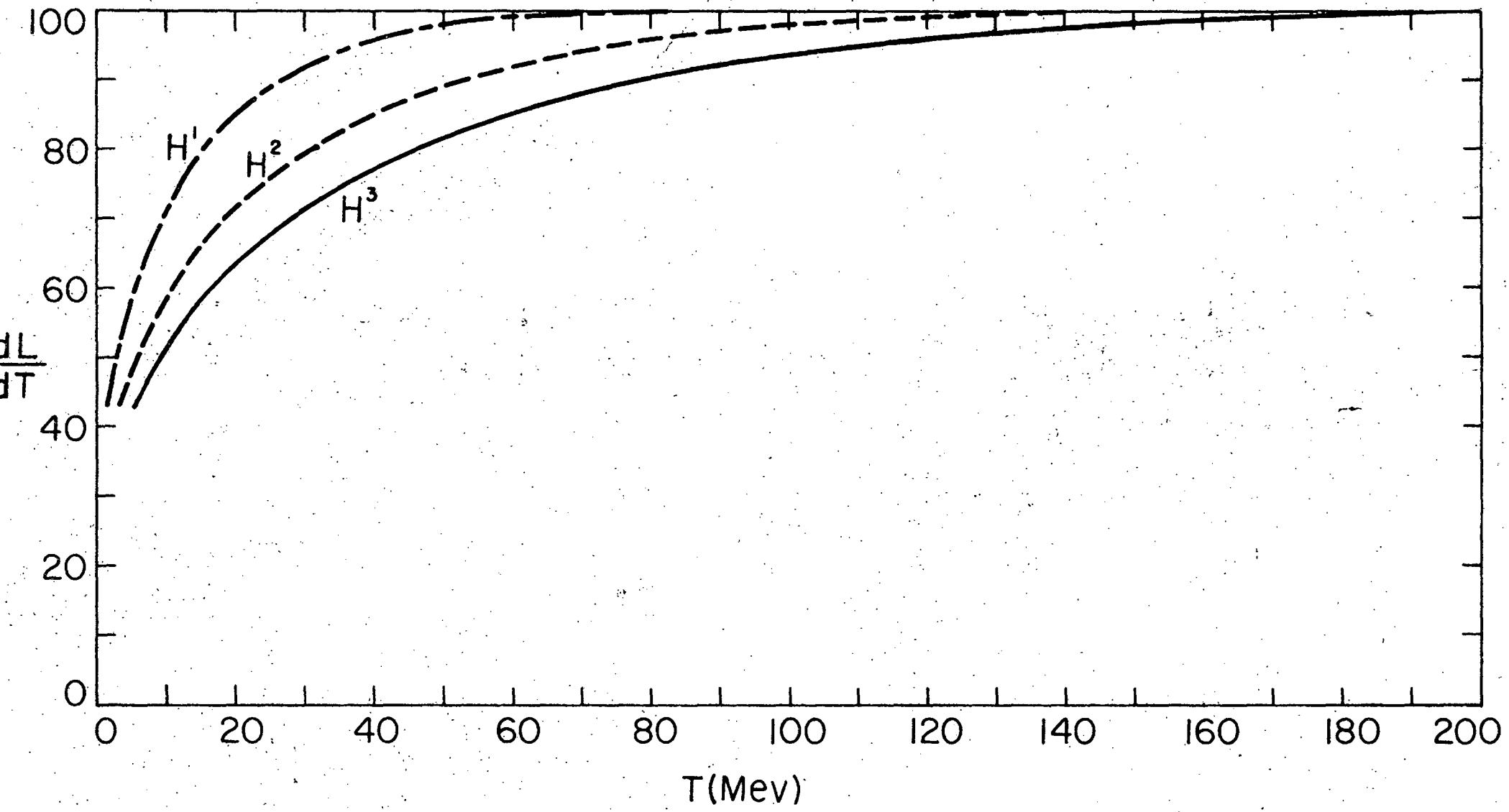
100
80
60
40
20
0
dL/dT
H¹
H²
H³
0
20
40
60
80
100
120
140
160
180
200
T(Mev)

Fig 9

23800-1

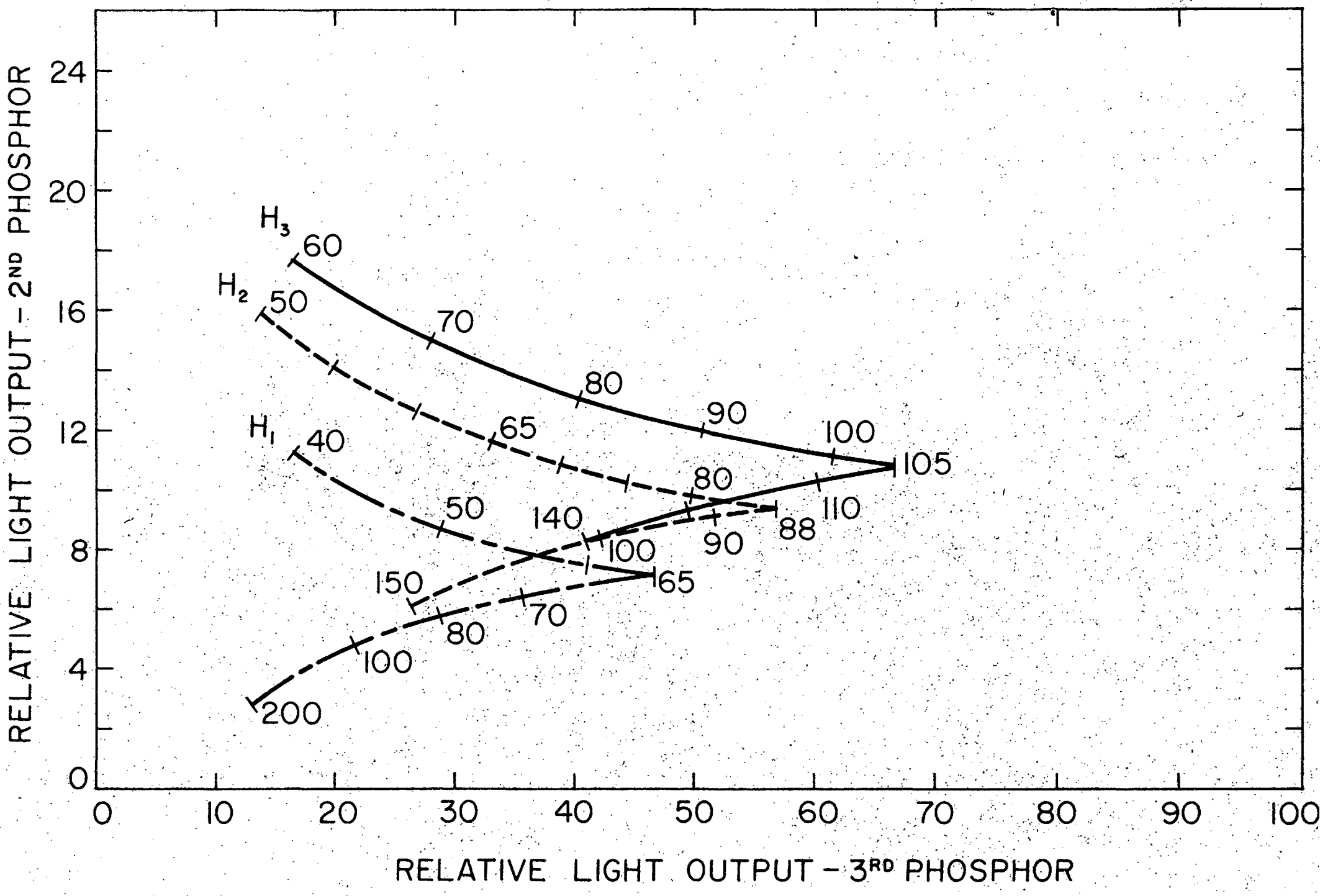

Fig 10

23802-1

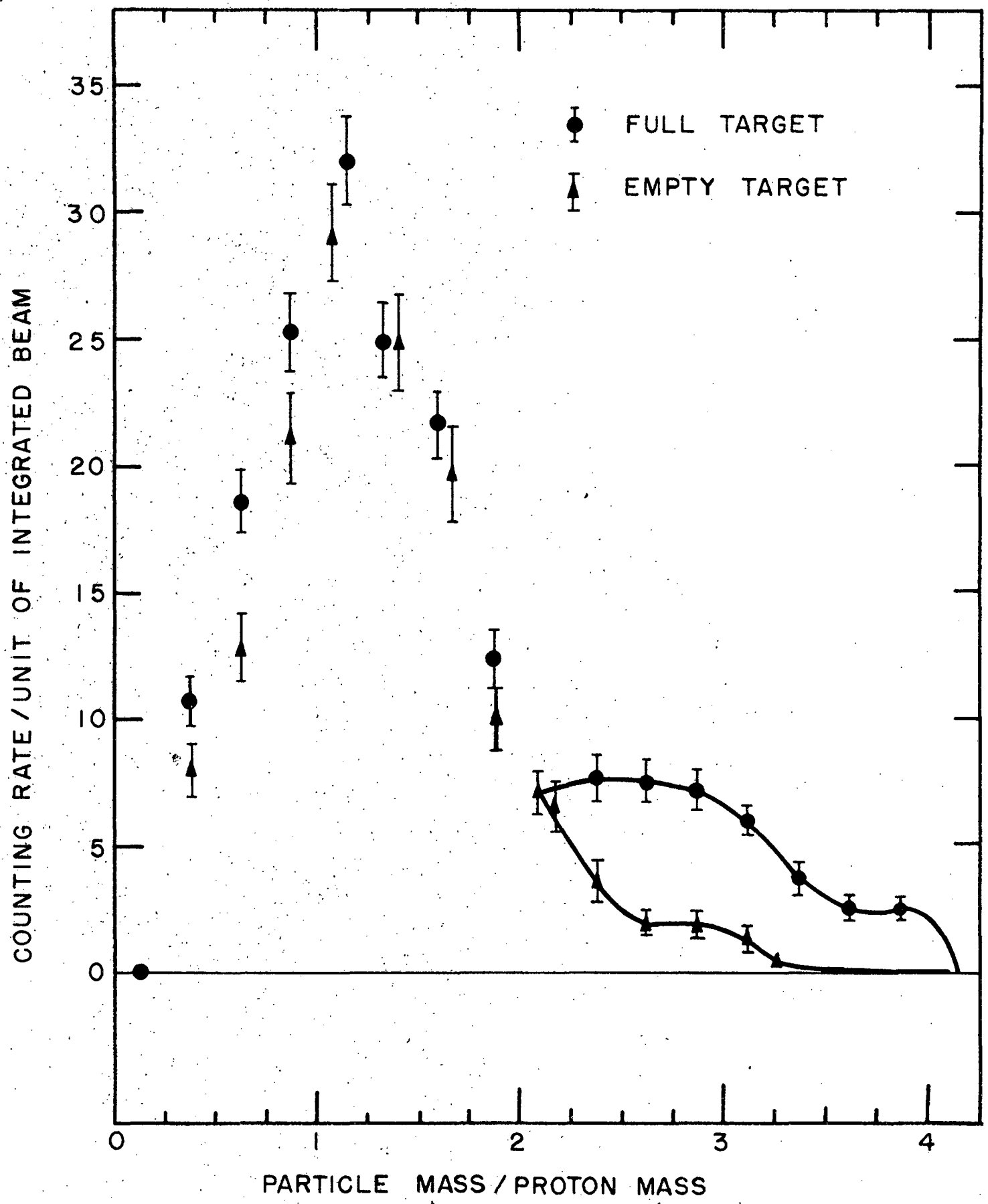
FULL TARGET
EMPTY TARGET
COUNTING RATE / UNIT OF INTEGRATED BEAM
35
30
25
20
15
10
5
0
0
1
2
3
4
PARTICLE MASS / PROTON MASS

22466-1

Fig 1

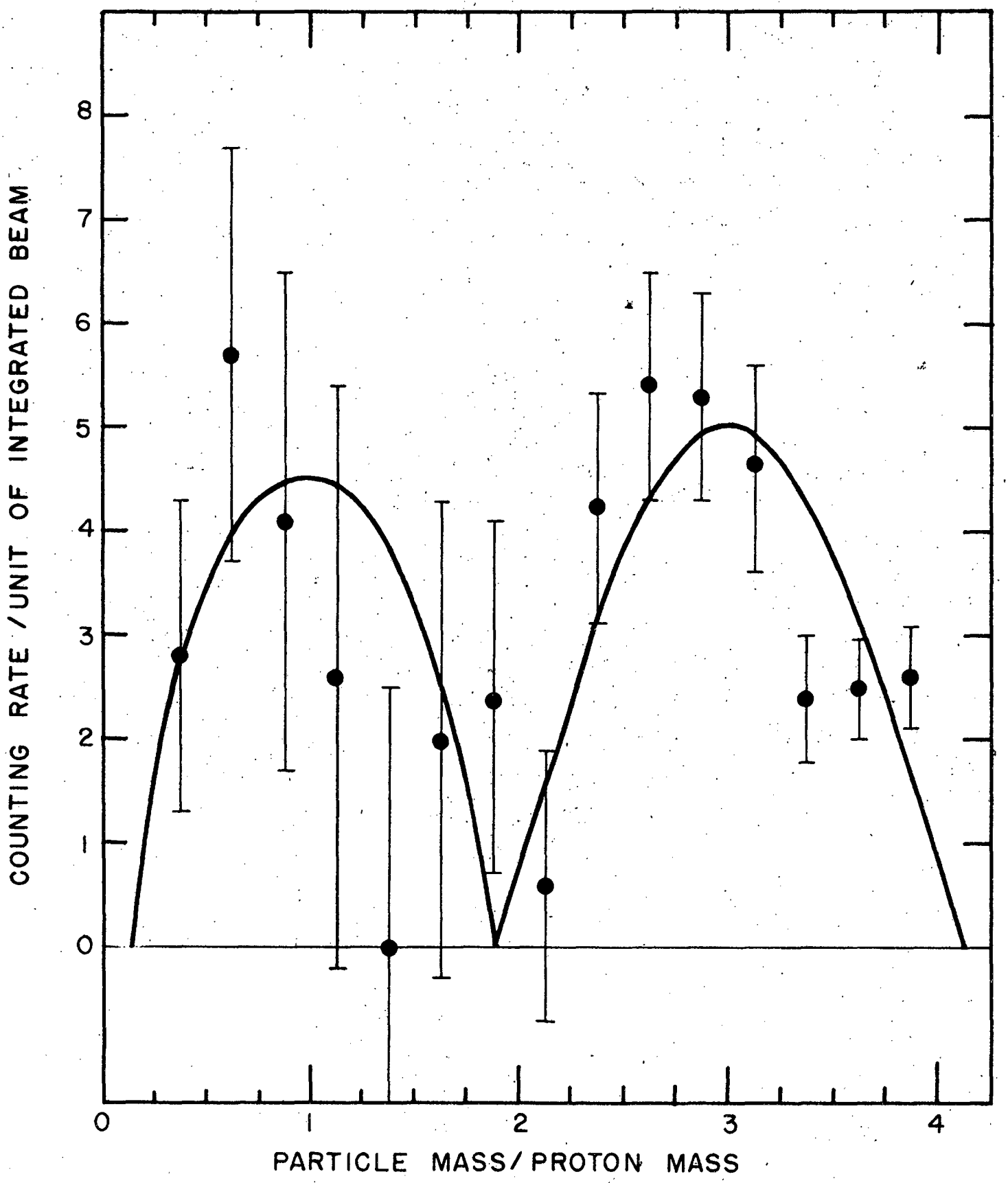

Fig 12

22465-1

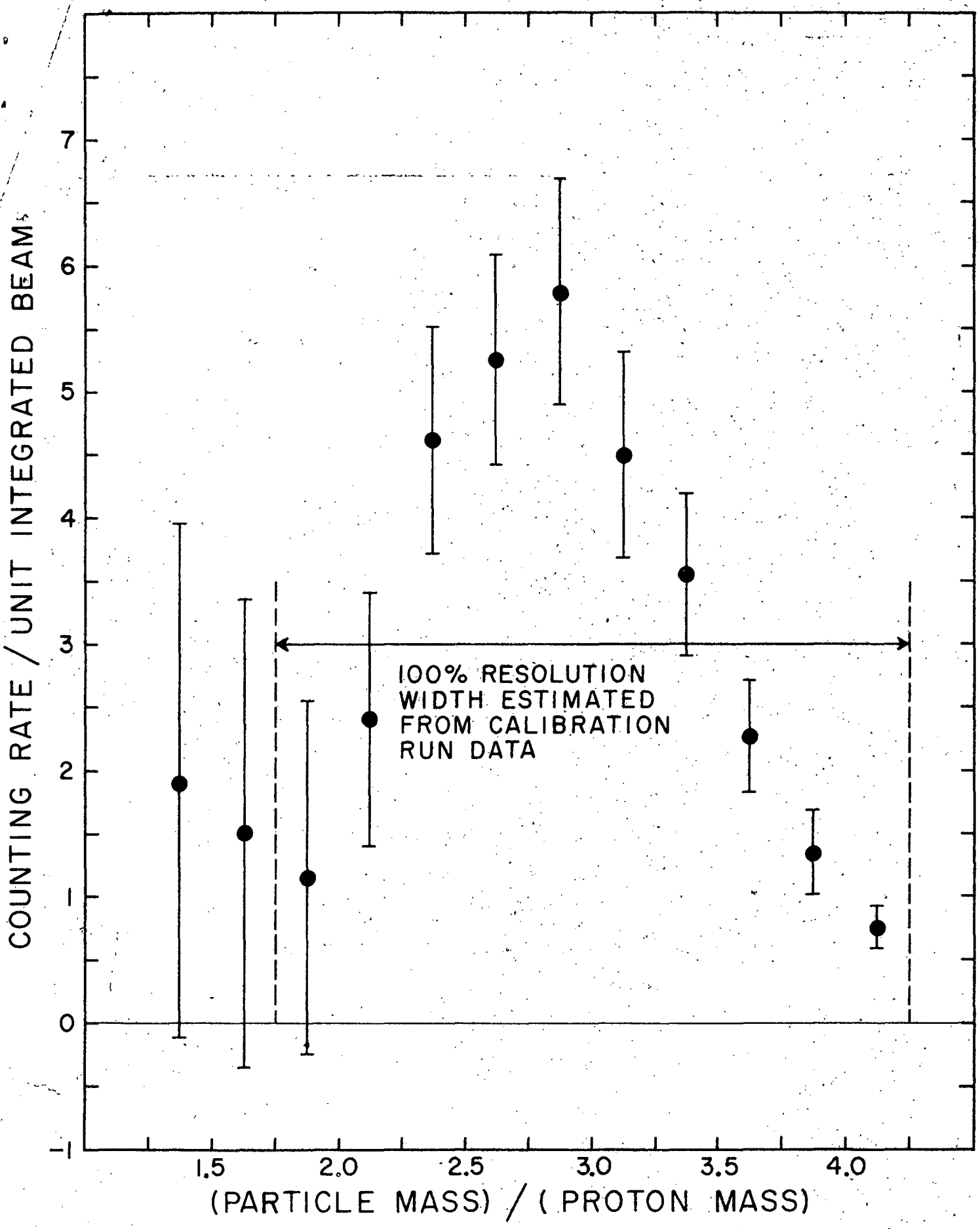

Fig 13

22525-1